Journal of Physics and Chemistry of Solids 120 (2018) 1–5

Contents lists available at ScienceDirect

Journal of Physics and Chemistry of Solids

journal homepage: www.elsevier.com/locate/jpcs

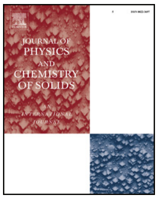

First-principles study of the optical properties of YPO_4 crystal with oxygen vacancies

Xiaoxiao Lu[a], Tingyu Liu[a,b,*], Mingxue Fu[a], Jing Li[a]

[a] College of Science, University of Shanghai for Science and Technology, Shanghai, 200093, China
[b] Shanghai Key Lab of Modern Optical System University of Shanghai for Science and Technology, Shanghai, 200093, China

ARTICLE INFO

Keywords:
Density functional theory
Electron–phonon coupling
Finite-size correction scheme alignment
Optical property
Oxygen vacancy

ABSTRACT

In this study, in order to obtain more accurate optical spectrum line shapes, the defect formation energies of oxygen vacancies in YPO_4 crystals with three different charges (0, +1, +2) were calculated using the finite-size correction scheme. The optical properties of the F center and F^+ center were studied based on electron–phonon coupling. The emission peak calculated for the F^+ center was close to the experimental value. The luminescence and absorption peaks were in the ultraviolet region for the F and F^+ centers. We predicted that the absorption peak at 140 nm was related to the F center and that at 152 nm to the F^+ center.

1. Introduction

YPO_4 crystals have many applications because of their high solid solubility, excellent chemical stability, and radiation resistance [1,2]. They are used in the manufacture of lasers, monitors, glass-ceramics, and other products [3–5]. In recent decades, scintillation crystals have attracted much attention and phosphates are potential scintillation crystals. In particular, YPO_4 crystals doped with different concentrations of rare earth ions can exhibit scintillation properties. The decay time of YPO_4:Ce^{3+} is about 23 ns, the decay time of YPO_4:Pr^{3+} is about 17 ns [6], and the decay time of YPO_4:Nd^{3+} is about 6 ns? The host YPO_4 doped with Nd^{3+} is a more promising activator in scintillator materials compared with YPO_4 crystals doped with other rare earth ions [7].

Doping YPO_4 with different concentrations of rare earth ions is an active research area and there are many methods for preparing these compounds, such as sol–gel [8], precipitation [9], and hydrothermal methods [10]. However, high-temperature sintering leads to the loss of P_2O_5 by evaporation during synthesis [11], and thus defects always exist, although ripeness methods have been employed to synthesize pure crystals and crystals doped with rare earth ions. The defects in Frenkel pairs of yttrium, phosphorus, and oxygen atoms were studied by Urusov et al. using molecular dynamics methods [12]. Gao et al. calculated the formation energies for intrinsic defects, including vacancies, interstitials, and antisite defects, in yttrium, phosphorus, and oxygen atoms under different O-rich, Y_2O_3-rich, and Y-rich conditions based on the density functional theory (DFT) [13]. However, corrections of the formation energies were not investigated in detail.

Saito et al. calculated the absorption value for the ${PO_4}^{3-}$ ion location in the region of 7 eV–10 eV [14]. Nakazawa et al. showed that the effective excitation band around the absorption edge of the host is due to the excitation of ${PO_4}^{3-}$ ions [15]. Kim et al. [16] studied the absorption peaks at 8.3 eV in samples prepared using the hydrothermal method and solid state reaction, Zhang et al. concluded that the absorption band located in the 142 nm region was due to the ${PO_4}^{3-}$ ion shifting to the high-energy area [17]. Wang et al. found that the host absorption band in the 152 nm region was due to ${PO_4}^{3-}$ anion molecules [18]. The dielectric constant of the YPO_4 crystal is 8.0 [19].

In this study, we investigated the alignments of the formation energies of the oxygen vacancies and the electron–phonon coupling effect. The line shapes of the luminescence spectrum were calculated accurately for oxygen vacancies using first-principles methods.

2. Computational approach

In this study, we calculated the formation energy of the oxygen vacancies within the DFT framework [20]. The interactions between ions and electrons were described using the projector augmented wave method [21]. All of the calculations were conducted with the Vienna ab-initio simulation package (VASP) [22] using the generalized gradient approximation (GGA) of Perdew, Burke, and Ernzerhof (PBE) [23]. The main parameters used in the calculations were as follows: a supercell with 96 atoms ($2 \times 2 \times 1$ supercell), $3 \times 3 \times 3$ k-points sampling in reciprocal space, and a kinetic energy cutoff of 500 eV. The main parameters were checked in convergence tests. The optimized lattice parameters for the unit YPO_4 crystal were: $a = b = 6.8817$ Å,

---

[*] Corresponding author. College of Science, University of Shanghai for Science and Technology, Shanghai, 200093, China.
E-mail address: liutyyxj@163.com (T. Liu).

https://doi.org/10.1016/j.jpcs.2018.04.018
Received 19 October 2017; Received in revised form 13 April 2018; Accepted 16 April 2018

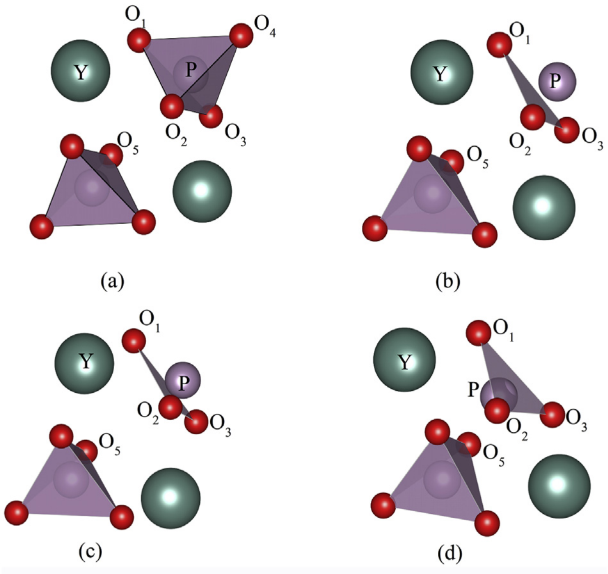

Fig. 1. (A) Structure of the components of the YPO_4 crystal, where (b), (c), and (d) represent the optimized structures of the YPO_4 crystal with $V_O^{\times}$, $V_O^{\bullet}$, and $V_O^{\bullet\bullet}$, respectively.

c = 6.0017 Å [24,25]. The convergence precision was 1×10^{-5} eV/atom, which was within the allowable error for calculating the total energy in the optimization process. The ISMEAR input command in VASP software was selected as −5 and we divided the Brillouin zone into tetrahedra. The oxygen vacancies were studied with three different charges (0, +1, +2).

3. Computational results and discussion

3.1. Structural optimization

After analyzing the optimized structures, the positions of the most adjacent Y atom, most adjacent P atom, and most adjacent O atoms surrounding the oxygen vacancy moved as shown in Fig. 1. The distances between the oxygen vacancy and neighboring atoms are listed in Table 1. $V_O^{\times}$ is the oxygen vacancy with neutral charge, $V_O^{\bullet}$ is the oxygen vacancy with singular positive charge, and $V_O^{\bullet\bullet}$ is the oxygen vacancy with double positive charges. Table 1 shows that the P atom shifted more in $V_O^{\bullet\bullet}$ than $V_O^{\bullet}$. The distances between the P atom and nearest O atom surrounding the oxygen vacancy under three different charges (0, +1, +2) were 1.6045 Å, 1.5385 Å, and 1.52039 Å, respectively, and the angles in the O_1-P-O_2 bonds were 107.6°, 115.3°, and 117.8°. In addition, the position of the P atom was close to the O_5 molecule and O_5 was a member of the tetrahedron in another $[PO_4{}^{3-}]$. Compared with the results obtained by Liu et al. [26], the Coulomb interaction between the P atom and the three O atoms was changed, where the length of the P-O bond was longer and this caused local distortion in $V_O^{\bullet\bullet}$. Thus, the Coulomb interaction between the P atom and oxygen vacancy was stronger in $V_O^{\bullet\bullet}$. These results are similar to those obtained for the oxygen atoms in a peroxyl bridge in silica [27].

Table 1
Distances between the oxygen vacancy and neighboring atoms.

Distance to V_O(Å)	Before relaxation	$V_O^{\times}$	$V_O^{\bullet}$	$V_O^{\bullet\bullet}$
Y-V_O	2.3951	2.3901	2.3999	2.4403
P-V_O	1.5546	1.3910	1.6207	2.5796
O-V_O	2.5917	2.5892	2.6123	2.7106
	2.4293	2.3946	2.4080	2.5233

3.2. Finite-size correction

The defect formation energies of point defects were calculated using the GGA. The defect formation energy can be determined by the follow equation [28]:

$$E_f = E^{DFT}(defecr + bulk) - E^{DFT} + \sum n_s\mu_s + q(E^{Fermi} + \varepsilon^{vbm} - \Delta v) - E_{correction}, \tag{1}$$

where the first two parts are the total energies of the bulk with and without the defect under DFT, respectively, $\Sigma n_s\mu_s$ is the chemical potential of the defect, i.e., oxygen, E^{Fermi} is the Fermi energy relative to the valence band maximum (VBM), ε^{vbm} is the VBM obtained from the bulk reference calculation, and ΔV refers to the average electrostatic potential difference between the bulk and the defect supercell [29]. The last part of this equation is the finite-size correction. When the supercell is added or electrons are taken out of the defect site, the error arises due to the non-physical self-image interactions between the electrons in neighboring cells. The whole supercell remains electrically neutral after introducing a uniform background charge [30]. According to Freysoldt et al. [28], $E_{correction}$ has two critical terms:

$$E_{correction} = E_q^{lat} - q\Delta_{q/0}, \tag{2}$$

where E^{lat} is the screened lattice energy under different charges q for the oxygen vacancy (+1, +2). The alignment term $\Delta_{q/o}$ can be obtained from the potential short-range v^{sr} [31] as follows:

$$q\Delta_{q/0} = \frac{1}{\Omega}\int d^3r V^{sr}(r), \tag{3}$$

$$V^{sr} = \widetilde{V}^{els}(ch\arg ed) - \widetilde{V}^{els}(neutral) - \widetilde{V}^{lr} + \Delta V, \tag{4}$$

where Ω is the volume of the supercell and $V^{\sim els}$ is the electrostatic potential. The average potential does not change between the neutral and charged defect, so the energy alignment term $\Delta_{q/o}$ is identical to the potential alignment term ΔV. The average potentials obtained using Eq. (4) for the neutral and charged defects are presented in Fig. 2. According to Freysoldt et al. [31], the long-range potential V^{lr} can be obtained from the model charge density q^{model} as follows.

$$V^{\mathrm{lr}}(r) = \int d^3r \frac{q^{\mathrm{mod}\,el}(r')}{\varepsilon(r - r')} \tag{5}$$

The long-range potential for the periodic array can be obtained from the Fourier transform of Eq. (5) as follows.

$$\widetilde{V}^{\mathrm{lr}}(G \neq 0) = \frac{4\pi q^{\mathrm{mod}\,el}(G)}{\varepsilon|G|^2},\ \widetilde{V}^{\mathrm{lr}}(0) = 0 \tag{6}$$

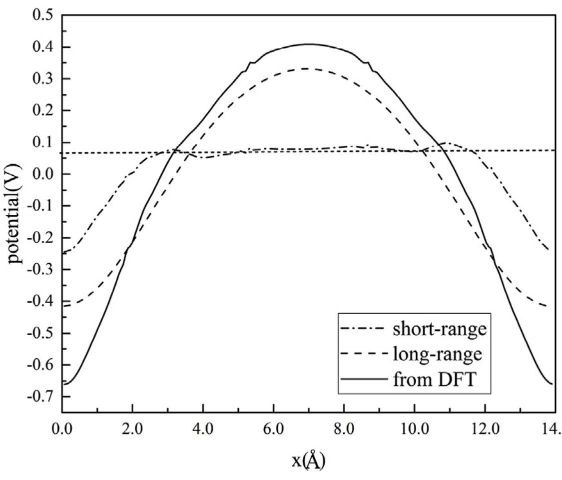

Fig. 2. Potentials for $V_O^{\bullet}$ in a 2 × 2 × 1 cubic YPO_4 supercell. The defect is located at x = 0 Å with a periodic image at x = 14 Å.